Generalized mean-field description of entanglement in dimerized spin systems

A. Boette, R. Rossignoli, N. Canosa, and J. M. Matera

Departamento de Física-IFLP, Universidad Nacional de La Plata, C.C. 67, La Plata (1900), Argentina
(Received 3 September 2014; revised manuscript received 10 February 2015; published 27 February 2015)

We discuss a generalized self-consistent mean-field (MF) treatment, based on the selection of an arbitrary subset of operators for representing the system density matrix, and its application to the problem of entanglement evaluation in composite quantum systems. As a specific example, we examine in detail a pair MF approach to the ground state (GS) of dimerized spin-1/2 systems with anisotropic ferromagnetic-type XY and XYZ couplings in a transverse field, including chains and arrays with first neighbor and also longer range couplings. The approach is fully analytic and able to capture the main features of the GS of these systems, in contrast with the conventional single-spin MF. Its phase diagram differs significantly from that of the latter, exhibiting (S_z) parity breaking just in a finite field window if the coupling between pairs is sufficiently weak, together with a fully dimerized phase below this window and a partially aligned phase above it. It is then shown that through symmetry restoration, the approach is able to correctly predict not only the concurrence of a pair, but also its entanglement with the rest of the chain, which shows a pronounced peak in the parity breaking window. Perturbative corrections allow to reproduce more subtle observables like the entanglement between weakly coupled spins and the low lying energy spectrum. All predictions are tested against exact results for finite systems.

I. INTRODUCTION

The analysis of correlations and entanglement in interacting quantum many-body systems has attracted strong attention in recent years [1,2], motivated by their deep implications for quantum information processing and transmission [3], the impressive advances in techniques for controlling and measuring quantum systems [4], and the new perspective they provide for the analysis of quantum phase transitions [1,2,5]. While the conventional mean-field (MF) approximations [6] provide a basic starting point for studying such systems over a broad range of the pertinent control parameters, they are not directly suitable for the description of entanglement, since they are based on completely factorized states. More sophisticated treatments have been developed to include and compute quantum correlations, like, for instance, density matrix renormalization group (DMRG) techniques [7,8], matrix product states, and tensor network methods [8–10], variational valence bond based approximations [11,12], quantum Monte Carlo calculations [13], and inclusion of static and quantum fluctuations around MF [14,15]. In addition, nonconventional MF approaches, able to intrinsically include some essential correlations, have also been proposed and recently improved and revisited [16–18], which start from the so-called cluster MF approach, also known as Bethe-Peierls-Weiss (BPW) approximation [19]. The essential point in these schemes is the consideration of composite sites containing more than one "body" as the basic independent units. Their application to specific spin systems [16,18] has shown their capability for determining phase diagrams and critical temperatures, as well as for describing the main features of observables such as magnetization and susceptibility. Their ability to predict entanglement measures has so far not been investigated.

The aim of this work is to investigate a general self-consistent variational MF treatment, based on the selection of an arbitrary subset of operators for representing the system density matrix [20], and its potential for describing basic entanglement measures in spin systems. The approach can be applied at both zero or finite temperatures and contains as particular cases the conventional as well as the cluster-type MF approaches. In contrast with other variational treatments, the generalized MF scheme does not require an explicit ansatz for the approximate GS, as the latter is naturally determined by the self-consistency relations according to the chosen set of operators. The scheme may be also used as a convenient starting point for more sophisticated treatments. We will examine, in particular, its capability for describing entanglement, both within the defined units as well as between them, the latter emerging through symmetry restoration or perturbative corrections.

As a specific example, we will consider a pair MF approximation to the ground state (GS) of dimerized spin-1/2 systems with anisotropic XY or XYZ couplings in a transverse field. In order to test its accuracy, we first examine the case of dimerized XY chains with first neighbor couplings, where the exact results for any size [21–26] can be obtained through the Jordan-Wigner fermionization [27]. We then examine dimerized chains with longer range couplings, dimer lattices and dimerized XYZ systems, where exact results for finite samples were obtained by numerical diagonalization. Dimerized systems are of great interest in both condensed matter physics and quantum information [21–26,28–33], and can be realized in different ways, including recently cold atoms trapped in optical lattices [34]. Spin-1/2 systems have the additional advantage of permitting a direct computation of the pairwise entanglement through the concurrence [35].

While conserving the conceptual simplicity of the conventional MF scheme, we will show that in contrast with the latter, the pair MF approach is able to provide a reliable yet still analytic and simple description of dimerized arrays. Its phase diagram differs significantly from that of the conventional MF, and clearly identifies, for a wide range of systems, a fully dimerized phase for weak fields, a partially aligned phase for strong fields and an intermediate S_z-parity breaking degenerate phase. It then predicts, in particular, the two transitions exhibited by the GS of the dimerized XY chain for increasing fields

[21], providing a clear approximate picture of the GS in each phase. The approach also leads to a reduced pair density which correctly describes not only the internal entanglement of the pair, but also (through symmetry restoration) its entanglement with the rest of the system, which shows a prominent peak precisely in the parity breaking sector. By means of simple perturbative corrections, the approach can predict the tails of this entanglement outside the parity breaking sector, as well as the entanglement between weakly coupled spins and the low lying energy spectrum. The formalism is described in Sec. II, while the application to dimerized XY and XYZ systems is developed in Sec. III, with the exact analytic solution for the dimerized XY chain discussed in the Appendix. Conclusions are given in Sec. IV.

II. FORMALISM

A. General self-consistent approximation

The mixed state ρ of a system at temperature $T = 1/k\beta$ described by a Hamiltonian H, minimizes the free energy functional $F(\rho) = \langle H \rangle_\rho - TS(\rho)$, where $\langle H \rangle_\rho = \mathrm{Tr}\,\rho H$ and $S(\rho) = -k\mathrm{Tr}\,\rho \ln \rho$ is the entropy. One can then formulate a general variational approximation to ρ based on the trial mixed state [20]

$$\rho_h = \exp(-\beta h)/Z_h, \quad h = \sum_i \lambda_i O_i, \qquad (1)$$

where $Z_h = \mathrm{Tr}\exp(-\beta h)$ and $\{O_i, i = 1, \ldots, m\}$ is an arbitrary set of linearly independent operators, with λ_i parameters determined through the minimization of $F(\rho_h)$. Considering the averages $\langle O_i \rangle \equiv \mathrm{Tr}\rho_h O_i$, functions of the λ_i's, as the independent parameters, the equations $\frac{\partial F(\rho_h)}{\partial \langle O_i \rangle} = 0$ lead to $\lambda_i = \frac{\partial \langle H \rangle}{\partial \langle O_i \rangle}$ and hence, to the *self-consistent* approximate Hamiltonian

$$h = \sum_i \frac{\partial \langle H \rangle}{\partial \langle O_i \rangle} O_i, \qquad (2)$$

where $\langle H \rangle = \mathrm{Tr}\,\rho_h H$. If the O_i's form a complete set, H is a linear combination of them and Eq. (2) leads to $h = H$. Otherwise, $\langle H \rangle$ will in general be a nonlinear function of the $\langle O_i \rangle's$ and (1) and (2) lead to a nonlinear set of equations for the $\lambda_i's$. While the basic MF approximations [6] are obtained when the O_i's are restricted to one-body operators and traces are taken in the grand canonical ensemble (with $H \to H - \mu N$), Eq. (2) holds for *any* restricted set, which may include *some* two-body (or in general n-body) operators, and for traces taken in *any* subspace $\mathcal{S}$ invariant under H and all $O_i's$ [20].

Here we will apply this general scheme to a composite system formed by N distinguishable subsystems, such as an array of spins s_i located at different sites, where the total Hilbert space is $\otimes_{i=1}^N \mathcal{S}_i$, with $\mathcal{S}_i$ that of subsystem i. We will consider Hamiltonians containing local terms and two-body couplings,

$$H = \sum_i B_\mu^i O_i^\mu - \frac{1}{2}\sum_{i \neq j} J_{\mu\nu}^{ij} O_i^\mu O_j^\nu, \qquad (3)$$

where O_i^μ are local operators pertaining to subsystem i ($[O_i^\mu, O_j^\nu] = 0$ if $i \neq j$) and sum over repeated labels μ, ν is implied. The standard MF arises when the O_i's in (1) and

(2) are restricted to *local* operators O_i^μ, i.e., when a "site" is identified with a *single* subsystem i. The present scheme enables, however, to consider as well *composite* sites C_k, such as pairs or clusters of spins in a spin system, where products $O_i^\mu O_j^\nu$ for sites i,j in the *same* cluster *are also included* within the operators O_i of (1) and (2). This is convenient when such pairs or clusters are internally strongly coupled but interact only weakly between them. The ensuing self-consistent scheme will treat the internal couplings exactly, leaving the MF for the weak couplings.

In this approach, $h = \sum_k h_k$, with h_k *local in C_k*, such that $\rho_h = \otimes_k \rho_k$, with $\rho_k = \exp(-\beta h_k)/Z_{h_k}$. Hence

$$\langle H \rangle = \sum_{k, i \in C_k} \left[B_\mu^i \langle O_i^\mu \rangle - \frac{1}{2}\sum_{j \in C_k} J_{\mu\nu}^{ij} \langle O_i^\mu O_j^\nu \rangle \right.$$
$$\left. - \frac{1}{2}\sum_{j \notin C_k} J_{\mu\nu}^{ij} \langle O_i^\mu \rangle \langle O_j^\nu \rangle \right], \qquad (4)$$

and Eq. (2) leads to

$$h_k = \sum_{i \in C_k} \left[\left(B_\mu^i - \sum_{j \notin C_k} J_{\mu\nu}^{ij} \langle O_j^\nu \rangle \right) O_i^\mu \right.$$
$$\left. - \frac{1}{2}\sum_{j \in C_k} J_{\mu\nu}^{ij} O_i^\mu O_j^\nu \right], \qquad (5)$$

which contains the exact internal two-body terms, as opposed to the standard MF. Equation (5) implies the self-consistent conditions

$$\langle O_i^\mu \rangle = \mathrm{Tr}\,\rho_k O_i^\mu, \quad i \in C_k, \qquad (6)$$

to be fulfilled for all C_k, which can be solved, for instance, iteratively, after starting from an initial guess for the $\langle O_i^\mu \rangle$'s or the associated parameters λ_μ^i. We will denote this approach as generalized MF (GMF). Equation (3) can now be rewritten as

$$H = \langle H \rangle + \sum_k \left[h_k - \langle h_k \rangle \right.$$
$$\left. - \frac{1}{2}\sum_{i \in C_k, j \notin C_k} J_{\mu\nu}^{ij} \left(O_i^\mu - \langle O_i^\mu \rangle \right)\left(O_j^\nu - \langle O_j^\nu \rangle \right) \right], \quad (7)$$

where the last term is the *residual interaction*.

For $T \to 0$, $\rho_k \to |0_k\rangle\langle 0_k|$, with $|0_k\rangle$ the GS of h_k. The present scheme will then lead in this limit to the state

$$|0_h\rangle = \otimes_k |0_k\rangle, \qquad (8)$$

which minimizes $\langle H \rangle \equiv \langle \Psi | H | \Psi \rangle$ among *all* cluster product states $|\Psi\rangle = \otimes_k |\psi_k\rangle$. Let us remark that an explicit ansatz for the states $|0_k\rangle$ is not required, since they can be obtained as the GS of h_k, Eq. (5), in each iteration. Nonetheless, in certain cases (see Sec. III) the explicit form of $|0_k\rangle$ may become apparent from the form of h_k and a direct minimization of $\langle H \rangle$ becomes feasible.

B. Perturbative corrections and symmetry restoration

While in-cluster correlations are already described by ρ_k or $|0_k\rangle$, those between clusters can in principle be estimated through perturbative corrections. At $T = 0$, it follows from Eq. (7) that H will connect $|0_h\rangle$ just with *two-cluster* excitations $|n_k n'_{k'}\rangle$, $k \neq k'$, $nn' \neq 0$, where $|n_k\rangle$ are the eigenstates of h_k ($h_k|n_k\rangle = \varepsilon_{n_k}|n_k\rangle$). Consequently, first-order (in the residual interaction) corrections will lead to the perturbed GS:

$$\left|0_H^1\right\rangle \propto |0_h\rangle + \sum_{k<k',n,n'\geqslant 1} \alpha_{kn,k'n'}|n_k n'_{k'}\rangle, \qquad (9)$$

$$\alpha_{kn,k'n'} = \sum_{i\in C_k, j\in C_{k'}} J_{\mu\nu}^{ij} \frac{\langle n_k|O_i^\mu|0_k\rangle\langle n'_{k'}|O_j^\nu|0_{k'}\rangle}{\varepsilon_{n_k} - \varepsilon_{0_k} + \varepsilon_{n'_{k'}} - \varepsilon_{0_{k'}}}, \qquad (10)$$

which contains just two-cluster excitations.

For instance, the reduced state of cluster k derived from (9) is ($\bar{k}$ denotes the complementary system)

$$\rho_k = \mathrm{Tr}_{\bar{k}}\left|0_H^1\right\rangle\!\left\langle 0_H^1\right| \propto |0_k\rangle\langle 0_k| + \sum_{n,m}(\alpha\alpha^\dagger)_{kn,km}|n_k\rangle\langle m_k|, \qquad (11)$$

which is a *mixed* state. Its entropy $S(\rho_k)$ represents the entanglement of the cluster with the rest of the system.

Beyond the weak coupling limit, the actual potential of the GMF lies in the possibility of breaking some essential symmetry of H, which will enable it to describe nonperturbative coupling effects between the composite sites. We will be here concerned with a discrete broken symmetry, namely spin-parity symmetry P_z (see next section), such that GMF will yield in some sectors a pair of parity breaking degenerate solutions $h_\pm$, with $h_- = P_z h_+ P_z$. We can then construct from the parity breaking GS $|0_{h_+}\rangle = \otimes_k|0_{k+}\rangle$ and $|0_{h_-}\rangle = P_z|0_{h_+}\rangle$, the definite parity states

$$|0_\pm\rangle = \frac{|0_{h_+}\rangle \pm |0_{h_-}\rangle}{\sqrt{2[1 \pm \mathrm{Re}(\langle 0_{h_+}|0_{h_-}\rangle)]}}, \qquad (12)$$

which will normally be not strictly degenerate in finite systems and which lead to a nonperturbative entanglement between composite sites: neglecting the complementary overlap $\prod_{k'\neq k}\langle 0_{k'+}|0_{k'-}\rangle$, typically small, the ensuing reduced state of the cluster k will be the same for $|0_\pm\rangle$ and given by

$$\rho_k = \mathrm{Tr}_{\bar{k}}|0_\pm\rangle\langle 0_\pm| \approx \tfrac{1}{2}(|0_{k+}\rangle\langle 0_{k+}| + |0_{k-}\rangle\langle 0_{k-}|), \qquad (13)$$

which is a rank-2 mixed state with eigenvalues

$$p_\pm = \tfrac{1}{2}(1 \pm |\langle 0_{k+}|0_{k-}\rangle|), \qquad (14)$$

and nonzero entropy $S(\rho_k)$. A parity breaking GMF is then a signature of a nonperturbative entanglement $S(\rho_k)$ between the composite site and the rest of the system in the exact (definite parity) GS. Similar considerations hold for a group G of clusters, for which the reduced state will again be a similar rank-2 mixed state with $p_\pm = \tfrac{1}{2}(1 \pm \prod_{k\in G}|\langle 0_{k+}|0_{k-}\rangle|)$. For a large group, $p_\pm \to 1/2$ and $S(\rho_G) \to \ln 2$. Such contribution is analogous to a "topological" entropy [36].
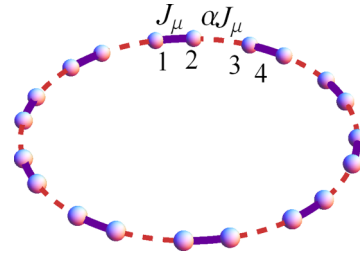

FIG. 1. (Color online) Schematic plot of the dimerized cyclic chain.

III. APPLICATION TO DIMERIZED SPIN SYSTEMS

A. Dimerized XY spin chain

We first consider a cyclic spin-$1/2$ chain of $N = 2n$ spins in a transverse uniform field B, coupled through alternating first-neighbor anisotropic XY couplings [21,22,24–26], such that the system can be viewed, at least for weak fields, as strongly coupled pairs weakly interacting with their neighboring pairs (Fig. 1). The Hamiltonian can be written as

$$H = \sum_{i=1}^{n} \left[B\left(s_{2i-1}^z + s_{2i}^z\right) - \sum_{\mu=x,y} J_\mu\left(s_{2i-1}^\mu s_{2i}^\mu + \alpha_\mu s_{2i}^\mu s_{2i+1}^\mu\right) \right], \qquad (15)$$

where s_i^μ denotes the (dimensionless) spin component at site i. We will focus on the case $\alpha_x = \alpha_y = \alpha$ (common anisotropy). We can suppose, without loss of generality, $|\alpha| \leqslant 1$ and, moreover, $\alpha \geqslant 0$, both in a cyclic chain ($s_{2n+1}^\mu = s_1^\mu$) with an even number n of pairs or in an open chain with n pairs, as its sign can be changed by a rotation of angle π around the z axis at even pairs (sites $2i - 1, 2i$, i even) [26]. A similar rotation at all even sites changes the sign of J_x and J_y, so that we can also assume $J_x \geqslant 0$, with $|J_y| \leqslant J_x$. We set here $|J_y| < J_x$. Finally, we set $B \geqslant 0$, as its sign can be changed by a global rotation of angle π around the x axis, which leaves the couplings unchanged. These arguments also hold for arbitrary spin s.

Equation (15) commutes with the total S_z parity

$$P_z = \exp[-i\pi(S_z + 2ns)], \qquad (16)$$

where $S_z = \sum_{i=1}^{2n} s_i^z$. This implies $\langle s_i^\mu\rangle = 0$ for $\mu = x, y$ in any nondegenerate eigenstate. Breaking of this symmetry ($\langle s_i^\mu\rangle \neq 0$ for $\mu = x$ or y) is, however, essential in MF descriptions, at least within some field intervals.

The conventional MF is based on a product state

$$\rho_h = \otimes_{i=1}^{2n}\rho_i, \quad \rho_i = \exp[-\beta h_i]/Z_{h_i}, \qquad (17)$$

where, for the chosen signs of couplings, we may assume all ρ_i identical in the cyclic case, such that $\langle s_i^\mu\rangle = \langle s^\mu\rangle$ and $\langle H\rangle = n[2B\langle s^z\rangle - (1 + \alpha)\sum_\mu J_\mu\langle s^\mu\rangle^2]$, with

$$h_i = \boldsymbol{\lambda}\cdot\boldsymbol{s}_i = Bs_i^z - (1 + \alpha)\sum_{\mu=x,y} J_\mu\langle s^\mu\rangle s_i^\mu \qquad (18)$$

Considering now $T = 0$, the GS $|0_i\rangle$ of h_i will be a state with maximum spin along $-\boldsymbol{\lambda}$, leading to $\langle s^z\rangle = -s\cos\theta$, $\langle s^x\rangle = s\sin\theta\cos\phi$, $\langle s^y\rangle = s\sin\theta\sin\phi$. Minimization of $\langle H\rangle$
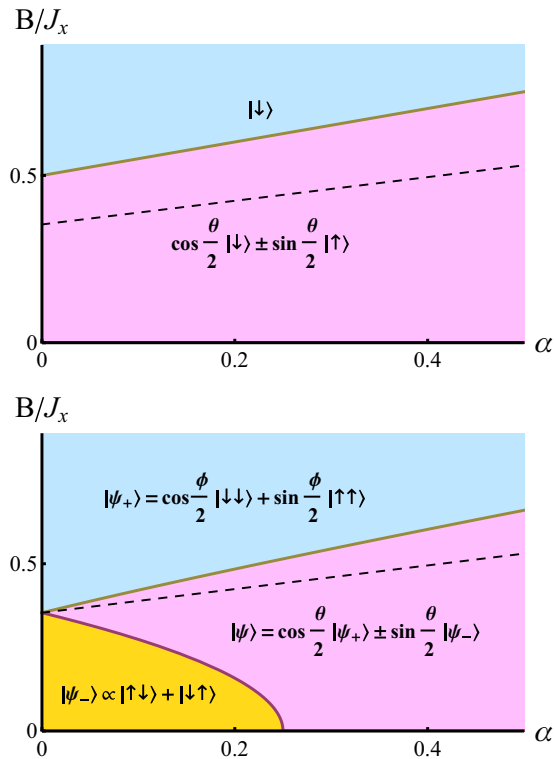
FIG. 2. (Color online) Phase diagram of the dimerized spin-1/2 chain according to the conventional (top panel) and pair (bottom panel) mean-field approaches, for $J_x > 0$ and $J_y = J_x/2$. The corresponding states for the unit cell are indicated. While in the conventional MF the S_z parity breaking phase arises below a critical field B_c^α, in the pair MF it occurs within a field window $B_{c1}^\alpha < B < B_{c2}^\alpha$ if $\alpha < \alpha_c$ [Eq. (33)]. For $B < B_{c1}^\alpha$, a dimerized state with maximally entangled pairs is preferred. The dashed lines denote the factorizing field B_s^α where both MF approaches coincide and are exact.

for $|J_y| < J_x$ leads then to $\phi = 0$ ($\langle s^y \rangle = 0$) and

$$\theta = 0, \quad B \geqslant B_c^\alpha \equiv J_x(1+\alpha)s, \\ \cos\theta = B/B_c^\alpha, \quad B < B_c^\alpha, \tag{19}$$

with parity broken for $B < B_c^\alpha$, where the solution is degenerate ($\theta = \pm|\theta|$). For $s = 1/2$, we then obtain

$$\langle 0_h|H|0_h \rangle = -n \begin{cases} B & B \geqslant B_c^\alpha \\ \frac{1}{2}\left(\frac{B^2}{B_c^\alpha} + B_c^\alpha\right) & B < B_c^\alpha \end{cases}, \tag{20}$$

where $|0_h\rangle = \otimes_{i=1}^{2n}|0_i\rangle$ with (Fig. 2)

$$|0_i\rangle = \cos\frac{\theta}{2}|{\downarrow}\rangle + \sin\frac{\theta}{2}|{\uparrow}\rangle. \tag{21}$$

This simple approach ignores the dimerized structure of the chain [it is the same as that for a chain with uniform coupling $J_x(1+\alpha)/2$], and is also blind to the weaker J_y coupling. Yet, it is remarkable that if $J_y \geqslant 0$, $|0_h\rangle$ does become an *exact* GS at the *separability field* [25,26,37–39]

$$B_s^\alpha \equiv \sqrt{J_y J_x}(1+\alpha)s = \sqrt{J_y/J_x}\, B_c^\alpha, \tag{22}$$

where $\cos\theta = \sqrt{J_y/J_x}$. At this field, the system exhibits a *degenerate* GS, with the GS subspace spanned by the

pair of degenerate MF product states [26,38]. No traces of dimerization are left at this point in the exact GS.

B. Pair mean-field approximation

In order to improve the conventional MF picture for $B \neq B_s^\alpha$, we now examine a generalized MF approach based on *independent spin pairs*, such that

$$\rho_h = \otimes_{i=1}^n \rho_i^p, \quad \rho_i^p = \exp\left(-\beta h_i^p\right)/Z_{h_i^p}, \tag{23}$$

with ρ_i^p a pair state. Equation (23) is exact in the fully dimerized limit $\alpha \to 0$, and can then be expected to provide a good approximation at least for small α. For the chosen signs of couplings, we may again assume all ρ_i^p identical in the cyclic case, with $\langle s_i^\mu \rangle = \langle s^\mu \rangle$, implying

$$\langle H \rangle = n\left[2B\langle s^z\rangle - \sum_{\mu=x,y} J_\mu\left(\langle s_1^\mu s_2^\mu\rangle + \alpha\langle s^\mu\rangle^2\right)\right] \tag{24}$$

and

$$h_i^p = B\left(s_{2i-1}^z + s_{2i}^z\right) \\ - \sum_{\mu=x,y} J_\mu[s_{2i-1}^\mu s_{2i}^\mu + \alpha\langle s^\mu\rangle(s_{2i-1}^\mu + s_{2i}^\mu)]. \tag{25}$$

For $|J_y| < J_x$, minimization of $\langle H \rangle$ leads again to $\langle s^y \rangle = 0$.

In the case of arbitrary spin and temperature, one should start from an initial seed for $\langle s^x \rangle$, diagonalize h_i^p and then recalculate $\langle s^x \rangle$ until convergence is reached. Considering now $T = 0$ and $s = 1/2$, it is apparent from (25) that the GS of h_i^p will be of the form

$$|0_i^p\rangle = \cos\frac{\theta}{2}\left(\cos\frac{\phi}{2}|{\downarrow\downarrow}\rangle + \sin\frac{\phi}{2}|{\uparrow\uparrow}\rangle\right) \\ + \sin\frac{\theta}{2}\frac{|{\uparrow\downarrow}\rangle + |{\downarrow\uparrow}\rangle}{\sqrt{2}}, \tag{26}$$

which is just the most general symmetric pair state real in the standard basis. Equation (24) becomes

$$\langle 0_h^p|H|0_h^p\rangle = -n\left[(B\cos\phi + J_-\sin\phi)\cos^2\frac{\theta}{2} + J_+\sin^2\frac{\theta}{2} \\ + \frac{1}{8}\alpha J_x \sin^2\theta(1+\sin\phi)\right], \tag{27}$$

where $|0_h^p\rangle = \otimes_{i=1}^n|0_i^p\rangle$ and $J_\pm = \frac{J_x \pm J_y}{4} \geqslant 0$. Minimization of $\langle H \rangle$ with respect to θ, ϕ can then be directly done, leading to

$$\theta = 0, \quad \tan\phi = \frac{J_-}{B}, \quad B \geqslant B_{c2}^\alpha, \tag{28a}$$

$$\begin{cases} \cos\theta = 2\frac{B\cos\phi + J_-\sin\phi - J_+}{\alpha J_x(1+\sin\phi)} \\ \tan\phi = \frac{J_- + \alpha J_x(1-\cos\theta)/4}{B}, \end{cases} \quad B_{c1}^\alpha < B < B_{c2}^\alpha, \tag{28b}$$

$$\theta = \pi \ (\phi \text{ arbitrary}), \quad B \leqslant B_{c1}^\alpha \tag{28c}$$

where the critical fields are given by

$$B_{c1}^\alpha = \frac{1}{2}\sqrt{J_x(J_y - 2\alpha J_x)},\tag{29}$$

$$B_{c2}^\alpha = \frac{1}{2}\sqrt{\left(J_+ + \frac{\alpha}{2}J_x + \sqrt{\left(J_+ + \frac{\alpha}{2}J_x\right)^2 + 2\alpha J_x J_-}\right)^2 - 4J_-^2},\tag{30}$$

as obtained from (28b) for $\theta \to 0$ and $\theta \to \pi$. The solution of system (28b) for θ and ϕ can in fact be determined analytically (it leads to a quartic equation for $\cos\phi$).

In contrast with the standard MF, it is first seen that a parity breaking solution ($\theta \in (0,\pi/2)$) will now arise just within a *field window* $B_{c1}^\alpha < B < B_{c2}^\alpha$ if α is sufficiently small and $J_y > 0$, as depicted in Fig. 2 (bottom panel). For $B < B_{c1}^\alpha$, the pair MF leads to a *fully dimerized phase*, where the strongly coupled pairs are in a $P_z = -1$ *Bell state* $\frac{|\uparrow\downarrow\rangle+|\downarrow\uparrow\rangle}{\sqrt{2}}$ and hence maximally entangled. On the other hand, for $B > B_{c2}^\alpha$, the approach leads to an entangled $P_z = 1$ pair state $\cos\frac{\phi}{2}|\downarrow\downarrow\rangle + \sin\frac{\phi}{2}|\uparrow\uparrow\rangle$, which is only partially aligned. The intermediate parity breaking phase (28b) is then a transition region between the previous opposite parity phases, in which the pair is in a combination of the previous states. In this region, the pair MF GS is twofold degenerate ($\theta = \pm|\theta|$). It is verified that the actual exact GS obtained from the Jordan-Wigner fermionization also exhibits two transitions for increasing positive fields [21] if α is sufficiently small, becoming in a finite chain nearly two-fold degenerate in the intermediate sector [25,26] and leading as well to almost maximally entangled pairs for low fields (see the Appendix and next section).

In the parity preserving phases, the pair MF GS energy obtained from (27) is just

$$\langle 0_h^p | H | 0_h^p \rangle = -n \begin{cases} \sqrt{B^2 + J_-^2}, & B \geqslant B_{c2}^\alpha \\ J_+, & B \leqslant B_{c1}^\alpha \end{cases},\tag{31}$$

which is, of course, lower than the conventional MF energy (20) in these intervals.

The factorizing field (22) lies within the parity breaking phase $\forall \alpha > 0$: $B_{c1}^\alpha < B_s^\alpha < B_{c2}^\alpha$. It is verified that at $B = B_s^\alpha$, Eq. (28b) leads to $\cos\theta = J_y/J_x$ and $\tan\phi = 2J_-/\sqrt{J_x J_y}$, implying

$$\tan^2\theta/2 = \sin\phi,\tag{32}$$

which is precisely the condition ensuring that the pair state (26) reduces to a product of single-spin states.

On the other hand, for $\alpha \to 0$ (where the pair MF becomes exact), B_{c1}^α and B_{c2}^α merge (Fig. 2), approaching both the $\alpha = 0$ factorizing field $B_s^0 = \sqrt{J_y J_x}/2$ ($B_{c1,2}^\alpha \approx B_s^0(1 \mp \alpha\frac{J_y}{J_x})$ for small α): the exact GS of an isolated pair undergoes, for $J_y > 0$, a sharp parity transition at $B = B_s^0$, from the Bell state $\frac{|\uparrow\downarrow\rangle+|\downarrow\uparrow\rangle}{\sqrt{2}}$ for $B < B_s^0$, with energy $-J_+$ [Eq. (31)] to the state $\cos\frac{\phi}{2}|\downarrow\downarrow\rangle + \sin\frac{\phi}{2}|\uparrow\uparrow\rangle$ for $B > B_s^0$, with energy $-\sqrt{B^2 + J_-^2}$. At $B = B_s^0$, these states become degenerate and coincide with the definite parity combinations (12) of the MF product states $\otimes_{i=1}^2 |0_i\rangle$.

It is also seen from Eq. (29) that B_{c1}^α vanishes for

$$\alpha = \alpha_c \equiv \frac{J_y}{2J_x}.\tag{33}$$

If $\alpha > \alpha_c$ (or $J_y < 0$) parity is broken for all $B \leqslant B_{c2}^\alpha$, as in the standard MF. Nonetheless, important differences with the latter persist: B_{c2}^α remains lower than the MF critical field B_c^α, even for $\alpha = 1$, and strongly coupled pairs remain entangled even for strong fields $B > B_c^\alpha$; full alignment occurs only for $B \to \infty$, with $\phi \approx J_-/B$ for $B \gg J_-$. The pair MF depends also on J_y, which affects the critical fields and the values of θ, ϕ.

If $J_y < 0$ (with $|J_y| \leqslant J_x$), B_{c2}^α also vanishes at $\alpha = -\frac{J_y}{2J_x} \geqslant 0$, entailing *no parity breaking phase* in the pair MF if $\alpha \leqslant -\frac{J_y}{2J_x}$. This is in qualitative agreement with the exact result (see Appendix), but differs from the standard MF, where parity breaking still occurs $\forall \alpha$.

If $J_x > 0$ but $\alpha < 0$, the pair MF state can be obtained by rotation of angle π around the z axis at *even* pairs of the $\alpha > 0$ pair state, which implies (ignoring in what follows overall phases) an *alternating* angle θ in (26) ($\theta_i = (-1)^i\theta$) in the parity breaking phase. If $\alpha > 0$ but $J_x < 0$ (with $|J_y| < |J_x|$), such rotation should be applied to all even sites, entailing $|\uparrow\downarrow\rangle + |\downarrow\uparrow\rangle \to |\uparrow\downarrow\rangle - |\downarrow\uparrow\rangle$ and $\cos\frac{\phi}{2}|\downarrow\downarrow\rangle + \sin\frac{\phi}{2}|\uparrow\uparrow\rangle \to \cos\frac{\phi}{2}|\downarrow\downarrow\rangle - \sin\frac{\phi}{2}|\uparrow\uparrow\rangle$ in (26).

C. Entanglement predictions and comparison with exact results

We first show in Figs. 3 and 4 typical GS results for different entanglement observables related with spin pairs and single spins in a finite chain with $n = 50$ pairs, according to conventional and pair MF as well as exact results (see Appendix). The latter correspond to the exact GS of the finite chain (having then a definite S_z parity).

For a pair of strongly coupled neighboring spins (1-2 in Fig. 1), the pair MF approach (23) leads, after the symmetry restoration (12) and (13), to the reduced state

$$\rho_{12}^{\rm GMF} = \begin{pmatrix} \cos^2\frac{\theta}{2}\sin^2\frac{\phi}{2} & 0 & 0 & \frac{1}{2}\cos^2\frac{\theta}{2}\sin\phi \\ 0 & \frac{1}{2}\sin^2\frac{\theta}{2} & \frac{1}{2}\sin^2\frac{\theta}{2} & 0 \\ 0 & \frac{1}{2}\sin^2\frac{\theta}{2} & \frac{1}{2}\sin^2\frac{\theta}{2} & 0 \\ \frac{1}{2}\cos^2\frac{\theta}{2}\sin\phi & 0 & 0 & \cos^2\frac{\theta}{2}\cos^2\frac{\phi}{2} \end{pmatrix}\tag{34}$$

(expressed in the standard basis) after neglecting the overlap $|\langle 0_i^p(\theta)|0_i^p(-\theta)\rangle|^{n-1}$ in the parity breaking phase. In this phase, it is a rank-2 mixed state (and is pure otherwise), with eigenvalues $(\sin^2\frac{\theta}{2}, \cos^2\frac{\theta}{2})$ [Eq. (14)]. It then leads within this phase to a *nonzero entanglement entropy* $E_{12} = S(\rho_{12})$
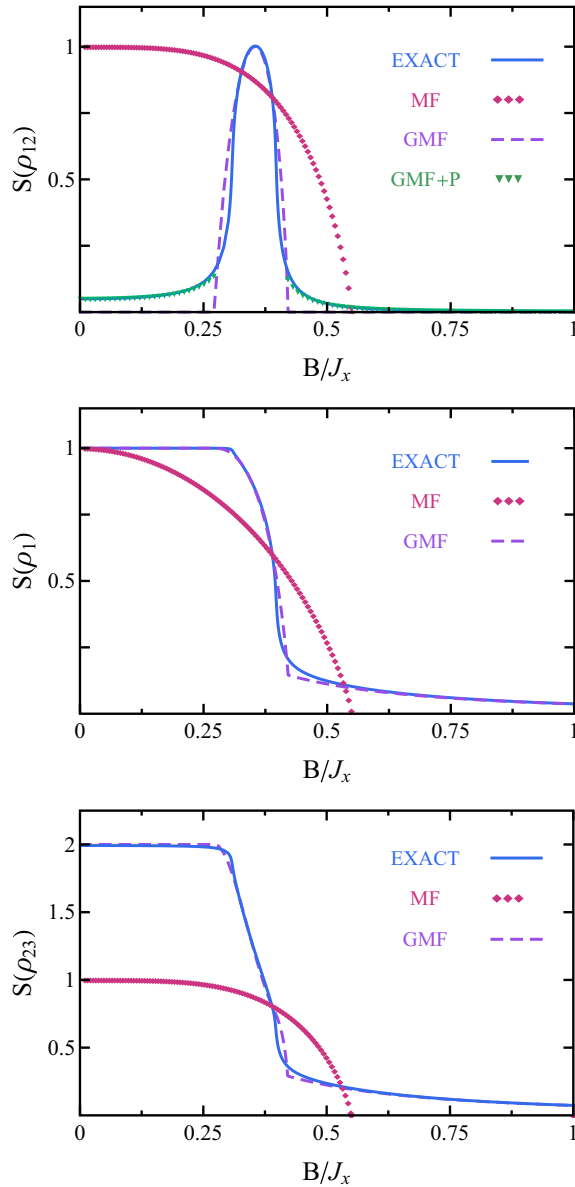
FIG. 3. (Color online) Exact and approximate results for the GS entanglement entropy of a strongly coupled spin pair (top), a single spin (center), and a weakly coupled neighboring pair (bottom), with the rest of the chain, for $\alpha = 0.1$ and $J_y/J_x = 1/2$, as a function of the (scaled) magnetic field. MF denotes the conventional single-spin MF treatment (17)–(21), while GMF the pair MF approach (23)–(26), both with symmetry restoration [Eq. (13)], and GMF+P the perturbed pair MF approach (9)–(11).
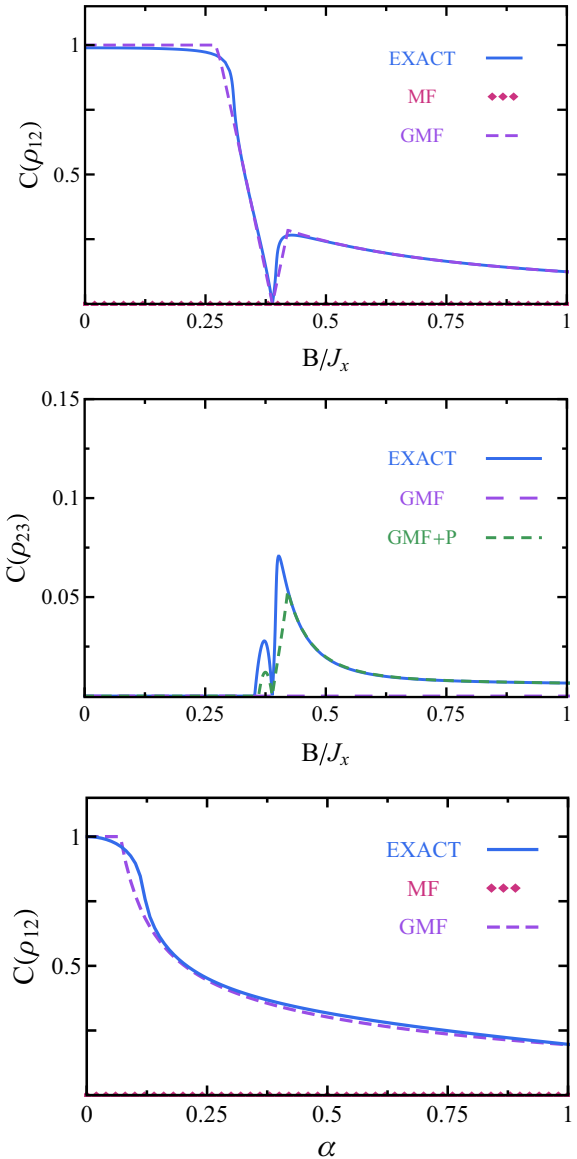

FIG. 4. (Color online) The concurrence of a strongly (top) and weakly (center) coupled pair of neighboring spins, as a function of the scaled magnetic field for the chain of Fig. 5, according to exact and approximate results. The bottom panel depicts the concurrence of a strongly coupled pair as a function of the weak coupling parameter α, at fixed field $B = 0.3J_x$. The standard MF result vanishes in all panels.

between the pair and the rest of the chain. As seen in the top panel of Fig. 3, this is in agreement with the exact result, which also exhibits a pronounced peak in this interval [we use $S(\rho) = -\text{Tr}\rho \log_2 \rho$ in all panels]. Parity breaking in the pair MF is then a signature of a *nonnegligible entanglement* between this pair and the rest of the chain. The exact result presents as well small nonzero tails outside the parity breaking interval, which can be correctly predicted by the *perturbed* pair MF reduced state (11).

Note that the entropy $S(\rho_{12})$ does not vanish as B approaches the factorizing field B_s^α ($\approx 0.39 J_x$ in Fig. 3), since

the exact GS remains with a definite parity (and hence entangled) in its immediate vicinity. In fact, for $B \to B_s^\alpha$, the result obtained from (34) becomes *exact* (except for the small neglected overlap), as the parity restored pair MF GS is exact in this limit. Actually, as stated before, at $B = B_s^\alpha$, the exact GS is degenerate, so that GS entanglement will depend at this point on the choice of GS. The result obtained from (34) corresponds to the definite parity GS's (12), which are the *actual side limits* [38] of the exact GS for $B \to B_s^{\alpha\pm}$.

The single-spin state derived from (34) is just

$$\rho_1^{\text{GMF}} = \begin{pmatrix} p_+ & 0 \\ 0 & p_- \end{pmatrix}, \quad p_\pm = \frac{1}{2}\left(1 \mp \cos^2\frac{\theta}{2}\cos\phi\right), \quad (35)$$

which is of the form $\frac{1}{2}(\rho_1^+ + \rho_1^-)$ in the parity breaking phase, with $\rho_1^{\pm}$ the single-spin reduced states derived from the pair state (26) before parity restoration. Its entropy, quantifying its entanglement with the rest of the chain, is nonzero for all fields and seen to be almost coincident with the exact result (center panel). It is obviously maximum in the dimerized phase $B < B_{c1}^{\alpha}$, but decreases rapidly in the parity breaking phase (when the pair becomes entangled with the rest of the chain) and slowly in the partially aligned phase $B > B_{c2}^{\alpha}$ (where $p_+ \approx \phi^2/4 = J_-^2/(4B^2)$). The result derived from (35) is again fully exact for $B \to B_s^{\alpha}$.

The entanglement entropy $S(\rho_{23})$ of a weakly coupled pair with the rest of the chain can again be correctly described by the pair MF approach, as seen in the bottom panel. Note that $\rho_{23}^{\mathrm{GMF}} = \frac{1}{2}(\rho_1^+ \otimes \rho_1^+ + \rho_1^- \otimes \rho_1^-)$, so that in the parity preserving phases ($\rho_1^+ = \rho_1^-$), $S(\rho_{23}^{\mathrm{GMF}})$ is just twice the single-spin entropy $S(\rho_1^{\mathrm{GMF}})$. This relation no longer holds, however, in the parity breaking phase.

In contrast, it is verified in all panels that the conventional MF (17) does not lead to a proper picture of any of these measures, even after symmetry restoration. The ensuing reduced pair state is the same for any pair,

$$\rho_{12}^{\mathrm{MF}} = \begin{pmatrix} \sin^4\frac{\theta}{2} & 0 & 0 & \frac{1}{4}\sin^2\theta \\ 0 & \frac{1}{4}\sin^2\theta & \frac{1}{4}\sin^2\theta & 0 \\ 0 & \frac{1}{4}\sin^2\theta & \frac{1}{4}\sin^2\theta & 0 \\ \frac{1}{4}\sin^2\theta & 0 & 0 & \cos^4\frac{\theta}{2} \end{pmatrix}, \quad (36)$$

which is a rank-2 state for $\theta \in (0,\pi)$ with eigenvalues $\frac{1 \pm \cos^2\theta}{2}$ [θ is here the MF angle (19)]. Its entropy does not reflect the exact entanglement of the strongly nor the weakly coupled pair. The associated single-spin reduced state is of the form (35) but with $p_{\pm} = (1 \mp \cos\theta)/2$, and cannot correctly reproduce either its entanglement with the rest of the chain (center panel in Fig. 3). It is seen, however, that there is one point where the conventional MF result is exact for all three quantities (i.e., where the MF curve crosses the exact curve), which is the factorizing field B_s^{α}. Here, the reduced states (36) and (34) become identical and, moreover, exact.

Figure 4 depicts the *concurrence* [35], a measure of the entanglement *between* the spins of a pair, for both strongly (1-2) and weakly (2-3) coupled pairs. In the first case, the pair MF state (34) leads to the concurrence

$$C(\rho_{12}^{\mathrm{GMF}}) = \left| \cos^2\frac{\theta}{2}(1 + \sin\phi) - 1 \right|, \quad (37)$$

which is parallel (as that in a state $|\uparrow\uparrow\rangle + |\downarrow\downarrow\rangle$) if the term within the bars is positive, i.e., $B > B_s^{\alpha}$, and antiparallel (as that in $|\downarrow\uparrow\rangle + |\uparrow\downarrow\rangle$) if this term is negative, i.e., $B < B_s^{\alpha}$, *vanishing* at the factorizing field B_s^{α} (see below). As seen in the top panel, the pair MF result shows again a very good agreement with the exact result for all fields, correctly predicting a maximally entangled pair for low fields $B < B_{c1}^{\alpha}$. Note that for $B < B_{c1}^{\alpha}$ and $B > B_{c2}^{\alpha}$, the state (34) is pure, implying that the pair MF concurrence is just a function of $S(\rho_1^{\mathrm{GMF}})$, and given by

$$C_{12}^{\mathrm{GMF}} = \begin{cases} 1 & , \quad B < B_{c1}^{\alpha} \\ \frac{J_-}{\sqrt{B^2 + J_-^2}} & , \quad B > B_{c2}^{\alpha} \end{cases}, \quad (38)$$

decreasing as J_-/B for strong fields $B \gg J_-$. However, in the parity breaking phase, the state (34) is mixed and the concurrence (37) is no longer a function of $S(\rho_1^{\mathrm{GMF}})$. In fact, and as opposed to the previous entropies, it *vanishes* at the factorizing field B_s^{α}, as can be verified from Eqs. (32) and (37), since state (34) becomes *separable* (a convex combination of product states [40]) at this point. Here the single spin ceases to be entangled with its partner (except for tiny overlap corrections) even though it remains entangled with the rest of the chain [$S(\rho_1^{\mathrm{GMF}}) \neq 0$], indicating again that no traces of dimerization remain.

We also mention that the fidelity [3] of the state (34) with the exact ρ_{12}, $F = \mathrm{Tr}\sqrt{\sqrt{\rho_{12}}\rho_{12}^{\mathrm{GMF}}\sqrt{\rho_{12}}}$, is very high ($\gtrsim 0.99$ for $\alpha = 0.1$ in all phases). In contrast, the conventional MF state (36) has a low fidelity, especially for $B < B_{c2}^{\alpha}$, and leads to a *zero* concurrence $\forall B$, since it is a separable state even after parity restoration ($\rho_{12}^{\mathrm{MF}} = \frac{1}{2}(\tilde{\rho}_1^+ \otimes \tilde{\rho}_1^+ + \tilde{\rho}_1^- \otimes \tilde{\rho}_1^-)$, with $\tilde{\rho}_1^{\pm}$ the MF single-spin state before parity restoration).

The concurrence of a weakly coupled neighboring pair is plotted in the central panel of Fig. 4. This quantity cannot be reproduced by the standard nor the pair MF, since even after parity restoration they lead to a separable state ρ_{23}. However, it can be correctly described by the reduced state $\rho_{23}^{\mathrm{GMF+P}}$ derived from the perturbed pair MF state (9). This concurrence is small and starts to be nonzero just before the factorizing field B_s^{α}, having peaks at both sides of B_s^{α}. We should actually recall that at the immediate vicinity of B_s^{α} (i.e., $B \to B_s^{\alpha\pm}$), the concurrence between *any* two spins acquires in a finite chain a common tiny yet nonzero value in the definite parity GS, which can be exactly predicted by both the conventional or pair MF after parity restoration if the overlap $|\langle\psi_{\theta\phi}|\psi_{-\theta\phi}\rangle|^{n-1}$ is conserved [26,38].

While the general accuracy of the pair MF approach will decrease as α increases, it will still improve the conventional MF results, even in the uniformly coupled case $\alpha = 1$. In the bottom panel of Fig. 4, we depict the pair MF concurrence of a strongly coupled pair for increasing α at a fixed field, which is seen to remain accurate for all $\alpha \leqslant 1$. The conventional MF result vanishes $\forall \alpha$.

D. Energy predictions

We plot in Fig. 5 some basic energy level predictions, in order to provide a general view of the pair MF approach. As seen in the top panel, the pair MF GS energy significantly improves the conventional MF result, especially for $B < B_s^{\alpha}$. In the bottom panel, we depict for clarity the first four excitation energies in a small chain of 8 spins ($n = 4$). According to the pair MF approach, the lowest levels are single pair excitations, of energies $E_m^0 = \varepsilon_m - \varepsilon_0$ [using the notation of Eq. (9)], which in the present case will be independent of the site and hence n-fold degenerate. It is verified that for small α, this is approximately the case. Moreover, the splitting of these levels due to the residual interaction can be correctly described by simple first order perturbative treatment. In the present cyclic case with a uniform pair MF, this leads to the perturbed pair excitation energies

$$E_m^{1k} = \varepsilon_m - \varepsilon_0 - 2\alpha \sum_{\mu=x,y} J_\mu \langle 0|s_1^\mu|m\rangle \langle m|s_2^\mu|0\rangle \cos\frac{2\pi k}{n}, \quad (39)$$
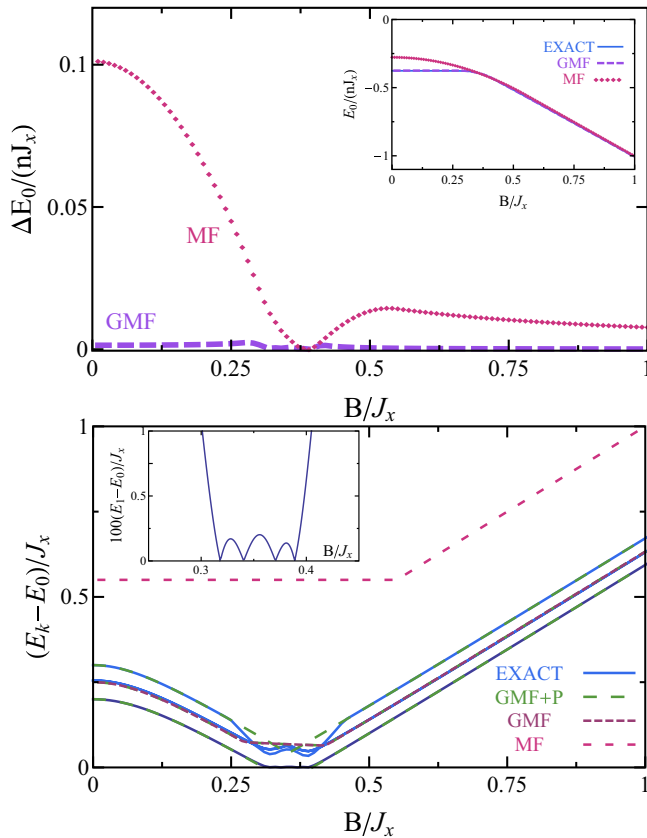
FIG. 5. (Color online) Top: The difference $\Delta E_0/n = (E_0^{\text{app}} - E_0^{\text{ex}})/n$ between the approximate and exact GS energies per pair, according to conventional and pair MF approaches, for the chain of Fig. 4. The inset depicts for reference the corresponding intensive GS energies. (Bottom) The first excitation energies of a small chain with 8 spins with the same parameters, according to pair MF and exact results. The inset depicts a blow up of the exact first excitation energy in the parity breaking region.

where ε_m are the eigenvalues of the single pair Hamiltonian (25) ($h^p|m\rangle = \varepsilon_m|m\rangle$), with ε_0 its GS energy, and $k = 1,\ldots,n$. These energies are those of the (discrete) Fourier transformed states $|\tilde{m}_k\rangle = \frac{1}{\sqrt{n}}\sum_{j=1}^{n} e^{i2\pi kj/n}|m_j\rangle$, where $|m_j\rangle$ denotes the state with pair j at excited level m. As seen in the bottom panel, the result obtained from (39) is practically exact in the parity preserving phases, where the energies ε_m are $\pm J_+$ and $\pm\sqrt{B^2 + J_-^2}$, and the lowest energies (39) become

$$E_1^{1k} = \pm(J_+ - \sqrt{B^2 + J_-^2}) - \alpha\left(J_+ + \frac{J_-^2}{\sqrt{B^2 + J_-^2}}\right)$$

$$\times \cos\frac{2\pi k}{n}, \qquad (40)$$

with $+$ for $B < B_{c1}^\alpha$ and $-$ for $B > B_{c2}^\alpha$. For $n = 4$, $E_1^{11} = E_1^{13} = E_1^0$, so that just three levels are seen. In contrast, the conventional MF leads to a single-spin excitation energy $E_1^{\text{MF}} = B$ for $B > B_c^\alpha$ and $J_x(1+\alpha)/2$ if $B < B_c^\alpha$, which lies well above the previous levels.

The parity-breaking phase of the pair MF approach is seen (bottom panel) to coincide approximately with the region where the exact GS of the finite chain becomes nearly

degenerate [21,22,25,26]. The exact lowest energy levels of each parity sector become very close in this interval, actually crossing at n fields (as seen in the inset), with the last crossing taking place exactly at the factorizing field B_s^α. This interval is enclosed by the fields B_{c1}^{ex} and B_{c2}^{ex} where the lowest quasiparticle energy of the Jordan-Wigner fermionized Hamiltonian vanishes (see Appendix).

E. Longer range couplings and lattices

The pair MF approach remains directly applicable to more complex situations where exact analytic results are no longer available. For instance, if adjacent dimers in Fig. 1 are further connected by second- and third-neighbor couplings $-\alpha_2 J_\mu s_i^\mu s_{i+2}^\mu$ (for spins like 1-3 and 2-4) and $-\alpha_3 J_\mu s_{2i-1}^\mu s_{2i+2}^\mu$ (for spins like 1-4), such that

$$H = \sum_{i=1}^{n}\left\{B\left(s_{2i-1}^z + s_{2i}^z\right) - \sum_{\mu=x,y} J_\mu\left[s_{2i-1}^\mu s_{2i}^\mu\right.\right.$$

$$\left.\left. + \sum_{j=1,2}\left(\alpha_j s_{2i}^\mu s_{2i+j}^\mu + \alpha_{j+1} s_{2i-1}^\mu s_{2i+j}^\mu\right)\right]\right\}, \quad (41)$$

the Jordan-Wigner transformation will no longer lead to a quadratic (and hence analytically solvable) fermionic Hamiltonian. However, it is seen from Eqs. (4) and (5) that the previous MF and pair MF expressions and phase diagram (Fig. 2) remain valid with the replacement

$$\alpha = \alpha_1 + 2\alpha_2 + \alpha_3, \qquad (42)$$

provided α_2 and α_3 are also positive (as α_1) or sufficiently small. The system of Eq. (41) is equivalent to a ladder-type dimer chain (Fig. 6, left). A uniform factorizing field will still exist in this system for common anisotropy [26,38] [$\alpha_j^\mu = \alpha_j \forall j$, as considered in (41)], which will be again given by Eq. (22) with the previous value of α. Similar considerations hold for longer range XY couplings.

The phase diagram of Fig. 2 also applies, at the pair MF level, to ferromagnetic-type XY dimer lattices like that of Fig. 6, right, described by the Hamiltonian

$$H = \sum_{i,j}\left\{B\left(s_{2i-1,j}^z + s_{2i,j}^z\right) - \sum_{\mu=x,y} J_\mu\left[s_{2i-1,j}^\mu s_{2i,j}^\mu\right.\right.$$

$$\left.\left. + \alpha_1 s_{2i,j}^\mu s_{2i+1,j}^\mu + \alpha_2\left(s_{2i-1,j}^\mu s_{2i-1,j+1}^\mu + s_{2i,j}^\mu s_{2i,j+1}^\mu\right)\right]\right\},$$
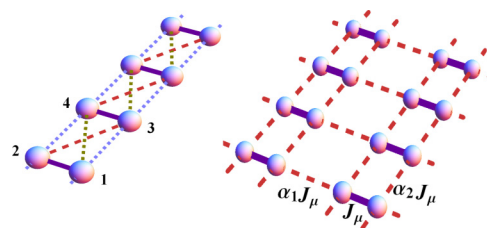
$$(43)$$

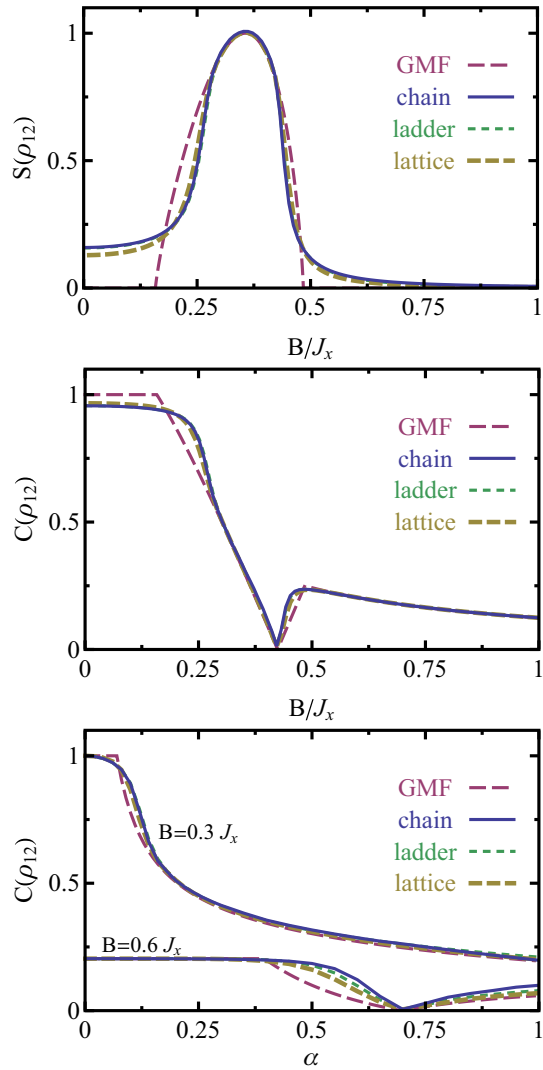FIG. 6. (Color online) The dimerized systems corresponding to Hamiltonians (41) (left) and (43) (right).

FIG. 7. (Color online) Results for the spin ladder and lattice of Fig. 6 [Eqs. (41) and (43)]. The entanglement of strongly coupled pairs with the rest of the system $S(\rho_{12})$ (top), and their concurrence $C(\rho_{12})$ (center), are plotted for increasing fields for a common value $\alpha = 0.2$ [Eqs. (42)–(44)]. Results for both systems are very close and almost coincident with those for the cyclic chain of Fig. 1, also depicted, in agreement with the common pair MF prediction (GMF). The bottom panel depicts the concurrence for increasing values of the total coupling parameter α, for two fixed values of the field.

where we assumed first neighbor couplings. For $\alpha_1 > 0$, $\alpha_2 > 0$, we should just replace

$$\alpha = \alpha_1 + 2\alpha_2, \tag{44}$$

in the MF and pair MF approaches. Similar considerations hold for 3D lattices or longer range couplings.

Figure 7 depicts illustrative results for a finite spin ladder and lattice with cyclic conditions [$n + 1 = n$ in (41), $n_i + 1 = n_i$ for $i = 1,2$ in (43)]. We have computed the exact results by exact diagonalization for a total of $2n = 16$ spins (2×8 ladder, 4×4 lattice). We have set a *fixed* value

$\alpha = 0.2$ in Eqs. (42) and (44), with $\alpha_1 = \alpha_2 = \alpha_3$ in (42) and $\alpha_1 = \alpha_2$ in (44). For comparison, results for the chain of Eq. (15) with the same α and spin number are also depicted.

It is verified that for a common total α, these systems do exhibit almost coincident values of the entanglement of a strongly coupled pair with the rest of the system, and of its concurrence, confirming the pair MF prediction. Moreover, the exact results are in very good agreement with the pair MF results. Those for the ladder are in fact almost indistinguishable from those of the chain, while those for the lattice are slightly closer to the pair MF result due to the larger connectivity, in agreement with the perturbative corrections of Eq. (11) [which can again predict the tails of $S(\rho_{12})$ in the parity preserving phases]. Conventional MF results, not shown, are similar to those of Figs. 3 and 4. The concurrence $C(\rho_{12})$ remains close in the three systems also for higher values of the total α, as seen in the bottom panel.

F. XYZ coupling

Let us now examine the effects of an additional J_z coupling in (3), i.e.,

$$H = \sum_{i=1}^{n} B\left(s_{2i-1}^z + s_{2i}^z\right) - \sum_{\mu=x,y,z} J_\mu\left(s_{2i-1}^\mu s_{2i}^\mu + \alpha_\mu s_{2i}^\mu s_{2i+1}^\mu\right). \tag{45}$$

As is well known, this model is no longer analytically solvable in the general anisotropic case (the added term does not lead to a quadratic fermionic operator in the Jordan-Wigner fermionization). We again assume $J_x > 0$ and $|J_y| < J_x$, with a common anisotropy $\alpha_\mu = \alpha > 0$.

For small values of J_z, the phase diagram of Fig. 2 remains essentially valid, with adequate shifts in the critical values of the field and α. At the conventional MF level, Eq. (19) applies with B_c^α replaced by the critical field

$$B_c^{\alpha z} = (J_x - J_z)(1 + \alpha)s,$$

with no parity breaking phase if $J_z > J_x$. And a uniform factorizing field still exists for common anisotropy if $J_z < J_y$, given by

$$B_s^{\alpha z} = \sqrt{(J_x - J_z)(J_y - J_z)}(1 + \alpha)s. \tag{46}$$

For $B = B_s^{\alpha z}$, the uniform parity breaking MF state (17)–(21) becomes again an exact degenerate GS [26], with $\cos\theta = \sqrt{\frac{J_y - J_z}{J_x - J_z}}$ (and $\theta = \pm|\theta|$). If $J_z > J_x > J_y$, a factorized eigenstate still exists at $B = B_s^{\alpha z}$, but will not be a GS [26].

At the pair MF level, we may still use the same state (26), which leads to

$$\langle 0_h^p | H | 0_h^p \rangle = \langle 0_h^p | H_{xy} | 0_h^p \rangle - \frac{n}{4} J_z \left(\cos\theta + \alpha \cos^2\phi \cos^4\frac{\theta}{2}\right), \tag{47}$$

where $\langle 0_h^p | H_{xy} | 0_h^p \rangle$ denotes Eq. (27). Hence, Eq. (28) are to be replaced by

$$\theta = 0, \quad \tan\phi = \frac{J_-}{B + \frac{1}{2}\alpha J_z \cos\phi}, \quad B \geqslant B_{c2}^{\alpha z}, \quad (48a)$$

$$\begin{cases} \cos\theta = \dfrac{2\left(B\cos\phi + J_-\sin\phi - J_+\right) + J_z\left(1 + \frac{1}{2}\alpha\cos^2\phi\right)}{\alpha\left(J_x(1+\sin\phi) - \frac{1}{2}J_z\cos^2\phi\right)} \\[2mm] \tan\phi = \dfrac{J_- + \frac{1}{4}\alpha J_x(1-\cos\theta)}{B + \frac{1}{4}\alpha J_z\cos\phi(1+\cos\theta)}, \end{cases} \quad B_{c1}^{\alpha z} < B < B_{c2}^{\alpha z}, \tag{48b}$$

$$\theta = \pi \ (\phi \text{ arbitrary}), \quad B \leqslant B_{c1}^{\alpha} \tag{48c}$$

where the critical fields depend now on J_z. The first critical field, which delimits the maximally entangled dimerized phase, has still a simple exact expression, given by

$$B_{c1}^{\alpha z} = \frac{1}{2}\sqrt{(J_x - J_z)(J_y - J_z - 2\alpha J_x)}. \tag{49}$$

Equation (49) implies that for $J_z < J_y$, this dimerized phase will exist for $\alpha < \alpha_{cz}$, with

$$\alpha_{cz} = \frac{J_y - J_z}{2J_x}. \tag{50}$$

If $\alpha > \alpha_{cz}$ (or $J_z > J_y$), parity will be broken for all $B < B_{c2}^{\alpha z}$. $B_{c2}^{\alpha z}$ will also vanish for sufficiently large J_z.

A positive J_z in Eq. (45) obviously increases the energy of the dimerized state [$\theta = \pi$ in Eq. (47)]. Hence its effect will be to decrease the critical fields, narrowing the dimerized phase as appreciated in Fig. 8. This phase will in fact disappear for $J_z > J_y - 2\alpha J_x$ [Eq. (49)], as also seen in Fig. 8. On the other hand, a negative J_z has the opposite effect, lowering the energy of the dimerized state and increasing $B_{c1}^{\alpha z}$, favoring dimerization. This picture will remain valid for sufficiently weak longer range XYZ couplings, employing the substitutions (42) or (44).

Results for a finite cyclic XYZ chain are depicted in Fig. 9. Exact results were again computed by diagonalization for $n = 16$ spins. It is verified that the pair MF predictions are fully confirmed. The addition of a small J_z coupling essentially
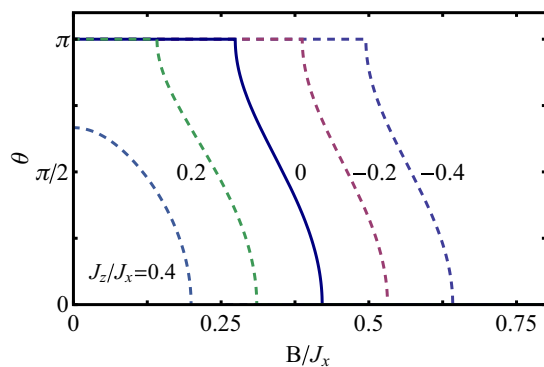
FIG. 8. (Color online) The angle θ of the pair MF approach for the XYZ Hamiltonian (45), as a function of the transverse field for different values of J_z/J_x. The dimerized phase corresponds to $\theta = \pi$, the partially aligned phase to $\theta = 0$ and the parity breaking phase to $0 < \theta < \pi$. We have set $J_y/J_x = 1/2$ and $\alpha = 0.1$. A positive (negative) J_z in (45) unfavors (favors) the dimerized phase, which will exist for $J_z < J_y - 2\alpha J_x$ [Eq. (50)].
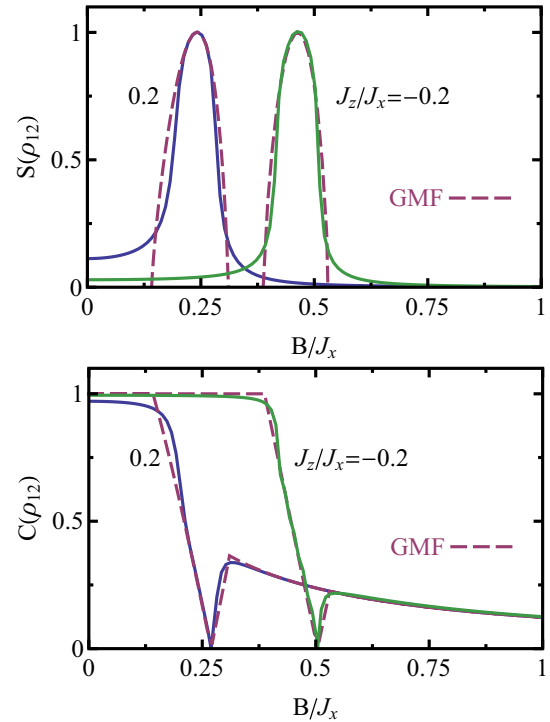
FIG. 9. (Color online) GS results for the XYZ chain of Eq. (45). The entanglement entropy $S(\rho_{12})$ (top) of strongly coupled pairs with the rest of the chain and their concurrence $C(\rho_{12})$ (bottom) are plotted for increasing fields at $\alpha = 0.1$ for $J_z = \pm 0.2J_x$. Exact results (solid lines) are again in agreement with those of the pair MF (GMF, dashed lines), which predicts a peak of $S(\rho_{12})$ in a displaced (with respect to that for $J_z = 0$) parity breaking sector, and a lower (higher) critical field for the dimerized phase if $J_z > 0$ ($J_z < 0$). The concurrence vanishes at the factorizing field (46).

shifts the results of the XY chain, in agreement with Eqs. (46) and (49). As previously stated, a reduced (extended) dimerized phase is obtained if $J_z > 0$ ($J_z < 0$), together with a displaced parity breaking phase, which is still clearly visible through the peak in the dimer entanglement entropy $S(\rho_{12})$ with the rest of the chain. There is again a good agreement with the pair MF results, which can also be improved by adding the corrections of Eq. (11). For strong fields $B \gg B_{c2}^{\alpha z}$, we mention that the final effect is the replacement $B \to B_{\text{eff}} = B + \frac{1}{4}\alpha J_z$ [Eq. (48a)], with $\phi \approx J_-/B_{\text{eff}}$ for $B \gg B_{c2}^{\alpha z}$.

IV. CONCLUSIONS

We have investigated a general self-consistent variational MF approximation, based on the selection of an arbitrary subset of operators for representing the system density matrix, and its capability for describing entanglement in the GS of composite systems. While retaining the conceptual simplicity of the conventional MF, the generalization allows to significantly improve it by considering composite cells, such that couplings within the cell are treated exactly. The approach is then specially suitable for systems where a partition in composite cells with strong internal couplings but weak cell-cell couplings is feasible, although it is not limited to this case.

In the dimerized systems considered, the approach naturally leads to a pair MF approximation which is still analytic and simple, but which goes well beyond the plain single-spin MF. Its phase diagram clearly identifies a dimerized phase for weak fields, together with a parity breaking phase in a transitional region between the latter and the strong field regime. The approach is thus able to accurately describe the entanglement of strongly coupled pairs, with parity breaking emerging as a signature of a non-negligible entanglement between these pairs and rest of system in the exact definite parity GS. With the addition of simple perturbative corrections, it is also possible to predict the concurrence of weakly coupled pairs and to improve the entanglement predictions, as well as to describe the main features of the energy spectrum.

The generalized MF can be used as a starting point for implementing more sophisticated techniques. It is also directly applicable at finite temperatures, higher spins, etc. These aspects and their application to more complex systems are currently under investigation.

APPENDIX: EXACT SOLUTION OF THE CYCLIC DIMER CHAIN

By means of the Jordan-Wigner transformation [27], and for a *fixed* value $P = \pm$ of the global S_z-parity P_z [Eq. (16)], we may exactly rewrite the dimerized Hamiltonian (15) as a quadratic form in standard fermion creation and annihilation operators $c_j^\dagger$, c_j, which in terms of the spin operators read

$$c_j^\dagger = s_j^+ \exp\left(-i\pi \sum_{k=1}^{j-1} s_k^+ s_k^-\right), \tag{A1}$$

where $s_j^\pm = s_j^x \pm i s_j^y$. These operators fulfill the fermionic anticommutation relations $[c_j, c_k^\dagger]_+ = \delta_{jk}, [c_j, c_k]_+ = 0$. The corresponding inverse transformation is

$$s_j^+ = c_j^\dagger \exp\left(i\pi \sum_{k=1}^{j-1} c_k^\dagger c_k\right). \tag{A2}$$

We then obtain, setting $J_\pm = \frac{J_x \pm J_y}{4}$,

$$H^P = \sum_{j=1}^{2n} B\left(c_j^\dagger c_j - \frac{1}{2}\right) \\ - \eta_j^P r_j (J_+ c_j^\dagger c_{j+1} + J_- c_j^\dagger c_{j+1}^\dagger + \text{H.c.}), \tag{A3}$$

where $r_j = \{^{1\ (j\ \text{odd})}_{\alpha\ (j\ \text{even})}$ and $\eta_j^+ = 1 - 2\delta_{j,2n}, \eta_j^- = 1$ in the cyclic case. Through separate parity dependent discrete Fourier transforms for even and odd sites,

$$\begin{pmatrix} c_{2j-1}^\dagger \\ c_{2j}^\dagger \end{pmatrix} = \frac{1}{\sqrt{n}} \sum_{k \in K_P} e^{-i2\pi kj/n} \begin{pmatrix} c'^\dagger_{k-} \\ c'^\dagger_{k+} \end{pmatrix},$$

where $K_+ = \{\frac{1}{2}, \ldots, n - \frac{1}{2}\}$, $K_- = \{0, \ldots, n-1\}$, we may rewrite (A3) as [26]

$$H^P = \sum_{k \in K_P} \left[\sum_{\sigma=\pm} B\left(c'^\dagger_{k\sigma} c'_{k\sigma} - \frac{1}{2}\right) \right. \\ \left. - (J_+^k c'^\dagger_{k-} c'_{k+} + J_-^k c'^\dagger_{k-} c'^\dagger_{-k+} + \text{H.c.}) \right] \\ = \sum_{k \in K_P} \sum_{\nu=\pm} \lambda_k^\nu \left(a_{k\nu}^\dagger a_{k\nu} - \frac{1}{2}\right), \tag{A4}$$

where $J_\pm^k = J_\pm(1 \pm \alpha e^{-i2\pi k/n})$ and $-k \equiv n - k$. The final diagonal form (A4) is obtained by means of a Bogoliubov transformation $c'^\dagger_{k\sigma} = \sum_{\nu=\pm} U_{k\sigma}^\nu a_{k\nu}^\dagger + V_{k\sigma}^\nu a_{-k\nu}$ determined through the diagonalization of 4×4 blocks:

$$\mathcal{H}_k = \begin{pmatrix} B & -J_+^k & 0 & -J_-^k \\ -\bar{J}_+^k & B & \bar{J}_-^k & 0 \\ 0 & J_-^k & -B & J_+^k \\ -\bar{J}_-^k & 0 & \bar{J}_+^k & -B \end{pmatrix}, \tag{A5}$$

whose eigenvalues are $\pm\lambda_k^+, \pm\lambda_k^-$, with

$$|\lambda_k^\pm| = \sqrt{\Delta \pm \sqrt{\Delta^2 - |B^2 - (J_+^k + J_-^k)(\bar{J}_+^k - \bar{J}_-^k)|^2}} \tag{A6}$$

and $\Delta = B^2 + |J_+^k|^2 + |J_-^k|^2$. Care should be taken to select the correct signs of $\lambda_k^\pm$ in order that the vacuum of the operators $a_{k\nu}$ has the proper S_z parity and represents the lowest state for this parity.

The spin correlations in the lowest states for each parity can then be obtained from the ensuing basic fermionic contractions $f_{ij} = \langle c_i^\dagger c_j \rangle - \frac{1}{2}\delta_{ij}, g_{ij} = \langle c_i^\dagger c_j^\dagger \rangle$, which can be directly obtained from the inverse Fourier transform of $\langle c'^\dagger_{k\sigma} c'_{k\sigma'} \rangle = \sum_\nu V_{k\sigma}^\nu \bar{V}_{k\sigma'}^\nu$, $\langle c'^\dagger_{k\sigma} c'^\dagger_{-k\sigma'} \rangle = \sum_\nu V_{k\sigma}^\nu U_{-k\sigma'}^\nu$. We then obtain, through the use of Wick's theorem, $\langle s_i^z \rangle = f_{ii}$, $\langle s_i^z s_j^z \rangle = f_{ii} f_{jj} - f_{ij}^2 + g_{ij}^2$, and $\langle s_i^\pm s_j^\mp \rangle = \frac{1}{4}[\det(A_{ij}^+) \pm \det(A_{ij}^-)]$, where $A_{ij}^\pm$ are $(j-i) \times (j-i)$ matrices of elements $2(f + g)_{i+p+0_1^0, i+q+1_0^1}$, with $p, q = 0, \ldots, j - i - 1$.

From Eq. (A6), it is seen that for real $B \neq 0$ and finite n, $|\lambda_k^+| > 0$ while λ_k^- vanishes just when $k = 0$ and

$$B = B_{c2}^{\text{ex}} = \frac{1}{2}\sqrt{(\alpha J_x + J_y)(J_x + \alpha J_y)}, \tag{A7}$$

or $k = n/2$ and

$$B = B_{c1}^{\text{ex}} = \frac{1}{2}\sqrt{(J_y - \alpha J_x)(J_x - \alpha J_y)}, \tag{A8}$$

remaining nonzero for other values of k. These critical fields coincide with those of Refs. [21,25] for the present situation. For $0 \leqslant \alpha \leqslant 1$ and $J_x > 0$, Eq. (A8) is real only for $J_y \geqslant 0$ and $\alpha \leqslant J_y/J_x$, while if $-J_x \leqslant J_y \leqslant 0$, Eq. (A7) is real for $\alpha \geqslant -J_y/J_x$. The pair MF critical fields (29) and (30) correspond approximately to these fields and satisfy

$$B_{c1} \leqslant B_{c1}^{\text{ex}} \leqslant B_s^\alpha \leqslant B_{c2}^{\text{ex}} \leqslant B_{c2}, \tag{A9}$$

for $J_y \geqslant 0$, all approaching the factorizing field $B_s^0 = \frac{\sqrt{J_x J_y}}{2}$ for $\alpha \to 0$ (where $B_{c1,c2}^{\text{ex}} \approx B_s^0[1 \mp \frac{\alpha}{2}(\frac{J_x}{J_y} + \frac{J_y}{J_x})]$).

The fields (A7) and (A8) enclose the interval where the finite chain GS will be almost twofold degenerate, i.e., where

the lowest state with positive S_z parity will have nearly the same energy as the lowest state with negative parity. Actually, starting at a field slightly above $B = B_{c1}^{ex}$, the exact GS of

the finite chain will experience n parity transitions [26,38] in the interval $(B_{c1}^{ex}, B_{c2}^{ex})$, with the last one taking place exactly at the factorizing field B_s^α.

[1] L. Amico *et al.*, Rev. Mod. Phys. **80**, 517 (2008).

[2] J. Eisert, M. Cramer, and M. B. Plenio, Rev. Mod. Phys. **82**, 277 (2010).

[3] M. A. Nielsen and I. L. Chuang, *Quantum Computation and Quantum Information* (Cambridge University Press, Cambridge, UK, 2000).

[4] S. Haroche and J. M. Raimond, *Exploring the Quantum* (Oxford University Press, Oxford, UK, 2006).

[5] T. J. Osborne and M. A. Nielsen, Phys. Rev. A **66**, 032110 (2002); G. Vidal, J. I. Latorre, E. Rico, and A. Kitaev, Phys. Rev. Lett. **90**, 227902 (2003).

[6] P. Ring and P. Schuck, *The Nuclear Many-body Problem* (Springer, Berlin, 1980); J. P. Blaizot and G. Ripka, *Quantum Theory of Finite Systems* (MIT Press, Cambridge, MA, 1986).

[7] S. R. White, Phys. Rev. Lett. **69**, 2863 (1992); U. Schollwock, Rev. Mod. Phys. **77**, 259 (2003); Ann. Phys. **326**, 96 (2011).

[8] S. Östlund and S. Rommer, Phys. Rev. Lett. **75**, 3537 (1995); S. Rommer and S. Östlund, Phys. Rev. B **55**, 2164 (1997).

[9] F. Verstraete, J. I. Cirac, and V. Murg, Adv. Phys. **57**, 143 (2008); F. Verstraete and J. I. Cirac, Phys. Rev. B **73**, 094423 (2006); J. I. Cirac and F. Verstraete, J. Phys. A **42**, 504004 (2009).

[10] G. Vidal, Phys. Rev. Lett. **99**, 220405 (2007); **101**, 110501 (2008); A. J. Ferris and G. Vidal, Phys. Rev. B **85**, 165147 (2012).

[11] S. Liang, B. Doucot, and P. W. Anderson, Phys. Rev. Lett. **61**, 365 (1988).

[12] J. Lou and A. W. Sandvik, Phys. Rev. B **76**, 104432 (2007); A. W. Sandvik and H. G. Evertz, *ibid.* **82**, 024407 (2010).

[13] W. M. C. Foulkes *et al.*, Rev. Mod. Phys. **73**, 33 (2001); R. J. Needs *et al.*, J. Phys. Condens. Matter **22**, 023201 (2010).

[14] R. Rossignoli and N. Canosa, Phys. Lett. B **394**, 242 (1997); R. Rossignoli, N. Canosa, and P. Ring, Phys. Rev. Lett. **80**, 1853 (1998); N. Canosa and R. Rossignoli, Phys. Rev. B **62**, 5886 (2000).

[15] N. Canosa, J. M. Matera, and R. Rossignoli, Phys. Rev. A **76**, 022310 (2007); J. M. Matera, R. Rossignoli, and N. Canosa, *ibid.* **78**, 042319 (2008); **82**, 052332 (2010).

[16] S. Mukhopadhyay and I. Chatterjee, J. Magn. Magn. Mater. **270**, 247 (2004).

[17] M. Dantziger, B. Glinsmann, S. Scheffler, B. Zimmermann, and P. J. Jensen, Phys. Rev. B **66**, 094416 (2002); I. Etxebarria, L. Elcoro, and J. M. Perez-Mato, Phys. Rev. E **70**, 066133 (2004).

[18] D. Yamamoto, Phys. Rev. B **79**, 144427 (2009); Y. Z. Ren, N. H. Tong, and X. C. Xie, J. Phys. Condens. Matter **26**, 115601 (2014).

[19] H. A. Bethe, Proc. R. Soc. London A **150**, 552 (1935); R. E. Peierls, Proc. Cambridge Philos. Soc. **32**, 477 (1936); P. R. Weiss, Phys. Rev. **74**, 1493 (1948); T. Oguchi, Prog. Theor. Phys. **13**, 148 (1955).

[20] R. Rossignoli and A. Plastino, Phys. Rev. A **42**, 2065 (1990); Phys. Rev. C **40**, 1798 (1989); R. Rossignoli, A. Plastino, and H. G. Miller, *ibid.* **43**, 1599 (1991).

[21] J. H. H. Perk, H. W. Capel, M. J. Zuilhof, and Th. J. Siskens, Phys. A **81**, 319 (1975); Th. J. Siskens, H. W. Capel, and J. H. H. Perk, Phys. Lett. A **53**, 21 (1975).

[22] J. H. H. Perk, H. W. Capel, and Th. J. Siskens, Phys. A **89**, 304 (1977); J. H. H. Perk and H. W. Capel, *ibid.* **92**, 163 (1978).

[23] J. H. H. Perk and H. Au-Yang, J. Stat. Phys. **135**, 599 (2009).

[24] E. I. Kutznetsova and E. B. Fel'dman, JETP Lett. **102**, 882 (2006); E. B. Fel'dman and M. G. Rudavets, *ibid.* **81**, 47 (2005); S. D. Doronin *et al.*, *ibid.* **85**, 519 (2007).

[25] G. L. Giorgi, Phys. Rev. B **79**, 060405(R) (2009); **80**, 019901(E) (2009).

[26] N. Canosa, R. Rossignoli, and J. M. Matera, Phys. Rev. B **81**, 054415 (2010).

[27] E. Lieb, T. Schultz, and D. Mattis, Ann. Phys. **16**, 407 (1961).

[28] C. K. Majundar and D. K. Gosh, J. Math. Phys. **10**, 1388 (1969); **10**, 1399 (1969); B. S. Shastry and B. Sutherland, Phys. Rev. Lett. **47**, 964 (1981).

[29] H. J. Schmidt, J. Phys. A **38**, 2123 (2005).

[30] D. Kaszlikowski, W. Son, and V. Vedral, Phys. Rev. A **76**, 054302 (2007).

[31] M.-G. Hu, K. Xue, and M.-L. Ge, Phys. Rev. A **78**, 052324 (2008).

[32] J. Sirker, A. Herzog, A. M. Oleś, and P. Horsch, Phys. Rev. Lett. **101**, 157204 (2008); A. Herzog, P. Horsch, A. M. Oleś, and J. Sirker, Phys. Rev. B **84**, 134428 (2011).

[33] P. Merchant *et al.*, Nat. Phys. **10**, 373 (2014).

[34] T. Ramos *et al.*, Phys. Rev. Lett. **113**, 237203 (2014); A. W. Glaetzle *et al.*, arXiv:1410.3388 [quant-ph]; I. Bloch, J. Dalibard, and W. Zwerger, Rev. Mod. Phys. **80**, 885 (2006).

[35] S. Hill and W. K. Wootters, Phys. Rev. Lett. **78**, 5022 (1997); W. K. Wootters, *ibid.* **80**, 2245 (1998).

[36] A. Kitaev and J. Preskill, Phys. Rev. Lett. **96**, 110404 (2006); M. Levin and X. G. Wen, *ibid.* **96**, 110405 (2006).

[37] S. M. Giampaolo, G. Adesso, and F. Illuminati, Phys. Rev. B **79**, 224434 (2009); Phys. Rev. Lett. **100**, 197201 (2008).

[38] R. Rossignoli, N. Canosa, and J. M. Matera, Phys. Rev. A **77**, 052322 (2008); **80**, 062325 (2009).

[39] J. Kurmann, H. Thomas, and G. Müller, Phys. A **112**, 235 (1982).

[40] R. F. Werner, Phys. Rev. A **40**, 4277 (1989).